Mitigation of charge injection in polyethylene films by silver nanoparticles/SiO_xC_y:H barrier layer: dependence on the particles size and surface density

Laurent Milliere, Gilbert Teyssedre*, Christian Laurent, Bernard Despax, Laurent Boudou and Kremena Maskasheva
LAPLACE (Laboratoire Plasma et Conversion d'Energie), Université de Toulouse; CNRS, UPS, INPT;
118 route de Narbonne, F-31062 Toulouse cedex 9, France
*Corresponding author: gilbert.teyssedre@laplace.univ-tlse.fr

***Abstract*— We have recently reported on the effect of silver nanoparticles plasma polymerized stack deposited on a polyethylene film preventing charge injection of both polarities under DC field. We investigate here the effects of the size and density of the silver nanograins on the barrier effect for charge injection. Size and density of the nanoparticles, and the surface coverage are controlled through the plasma process. A comparative study of space charge distribution between a reference polyethylene film and tailored films is presented in 300 µm-thick films using the pulsed-electroacoustic technique. It is shown that the barrier effect depends on the size distribution of the nanoparticles and surface coverage: 15 nm silver nanoparticles with a high surface density but still not percolating form an efficient barrier layer that suppress charge injection. It is worthy to note that charge injection is detected with an increasing intensity for percolating nanoparticles, for a semi-insulating layer without nanoparticles and for smaller size silver particles (<10 nm). The mechanism of charge injection mitigation is discussed.**

Keywords—polyethylene, nanocomposite, silver nanograin, HVDC, charge injection, space charge mitigation.

I. INTRODUCTION

Space charge in polyethylene-based materials still constitutes a problem affecting the reliability of High Voltage Direct Current -HVDC lines [1, 2]. This phenomenon creates an internal electric field distribution different from the design field that can trigger local damages to the polymer structure leading ultimately to breakdown [3, 4]. Attempts are currently ongoing in different labs for reducing the amount of space charge acting either at the source of the charges or at the level of their dispersion in the material. Most of the researches concern the modification/improvement of bulk material by dispersion of nano fillers into the polymer bulk [5]. To our knowledge, few studies focus on the polymer/electrodes interface properties to limit charge injection effect. Tailoring the interfacial properties of the insulation could be a way to control the generation of electronic carriers. The most common studies consist in a modification of the polymer film interface by fluorination with a F_2/N_2 mixture [6]. Charge injection mitigation was reported to be due to the presence of deep traps into the fluorinated layer that can block or shield further charge injection. Following a different strategy, we recently reported [7] on charge injection mitigation when a thin composite layer containing silver nanoparticles (AgNPs) was deposited on the surface of polyethylene as shown in Figure 1. A drastic effect was observed and attributed to the presence of AgNPs acting as deep traps. In this paper, we extend the analysis in order to find out what features of the nanocomposite layer are playing a key role in charge injection mitigation.

This work is financially supported by the Agence Nationale de la Recherche in France, project ANR-InTail under contract ANR-AA-PBLI-II-2011.

II. EXPERIMENTAL AND ANALYSIS

A. Substrate preparation

Polymer films of additive-free low density polyethylene (LDPE from BOREALIS) were produced from pellets press-molded at 155°C under 3 bars for 20 minutes. The final samples were disks of 7 cm in diameter and 300 ± 10 µm in thickness. The films were subsequently outgassed for 12 h under vacuum (0.06 Pa) at 20°C for removing volatile molecules and water. No oxygen groups were observed on the LDPE samples after the preconditioning procedure [8]. Indeed it has been shown that even using additive-free polyethylene films, space charge can be detected originating from the material bulk and giving rise to spurious effect when investigating charge injection from the electrodes. When conditioning the samples under vacuum for some hours, injection phenomena can be observed as homo charge (charge of the same sign as the nearby electrode) above a field level of the order of 10 to 15 kV/mm using conventional space charge detection techniques [9]. This preconditioning also conforms to low pressure plasma deposition process described below.

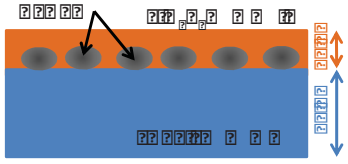

Fig. 1: Schema of polymer surface tailored by a AgNPs/SiO_xC_y:H nanocomposite barrier

B. RF plasma process and silver clusters characteristics

The nanocomposite layer is synthetized in a radio-frequency low pressure plasma reactor enabling sputtering from a silver target and plasma polymerization of

hexamethyldisiloxane (HMDSO $[CH_3]_6Si_2O$) as two independent steps in the same chamber [10, 11]. In a first step, AgNPs are deposited onto the surface of the LDPE film. A range of parameters were chosen for deposition of the AgNPs as being 40, 60 and 80 W for the discharge power, 5.33 and 8.00 Pa for the discharge pressure, the deposition time being constant (5 s). These conditions lead to different shape, size and surface coverage of the AgNPs as specified in Table I. Going from low to high input power in the discharge, one obtains small (10 to 15 nm) and isolated AgNPs to large (20 to 30 nm) and percolated particles. The electrical properties of an assembly of nanoclusters dispersed in a dielectric matrix (SiO_xC_y:H layer in our case) change drastically at the percolation threshold where Ag islands form an infinite metallic cluster which spans the whole sample. Below the percolation threshold, charge transport is controlled by grain to grain thermally-activated tunneling whereas metallic conduction becomes predominant above [12]. In a second step, HMDSO is introduced into the chamber and the SiO_xC_y:H layer is deposited, covering the AgNPs previously formed at the PE surface and filling the space between them (deposition time is fixed at 60 s in our study).

C. Space charge measurements and barrier effect

The Pulsed Electro Acoustic (PEA) technique was used for space charge measurements [13]. The composite samples are sandwiched between the two electrodes of the PEA system (semiconducting –SC electrode connected to the voltage supply, aluminum electrode to the ground) without further metallization. The PEA test cell is installed in a thermo-stated oven and all measurements were realized at 25°C. To obtain an exploitable signal, the acoustic response to excitation by 600 V amplitude pulses at 1 kHz frequency is averaged for 60 s. The spatial resolution of the set-up is 25 µm. Deconvolution of the signal was done by software developed in our laboratory. The samples were tested following a protocol depicted in Fig. 2. It consists of different steps of polarization, each followed by a depolarization period. In a short term protocol (Fig. 2a) the applied stress is increased from 10 kV/mm to 50 kV/mm by steps of 5 kV/mm. The voltage is maintained at each step for 20 min, followed by a depolarization step for 20 min. After the last step at 50 kV/mm, the stress polarity was reversed to -40 kV/mm with a subsequent increase to -50 kV/mm. PEA profiles were recorded every 60 s in the polarization and depolarization steps at each voltage level. In a longer term protocol (Fig. 2b) we used two steps of 20 kV/mm and 40 kV/mm applied for 12 hours each. Each step is followed by a depolarization period lasting for 5 hours. PEA profiles were recorded every 150 s. The dynamics of the space charge is illustrated through color maps showing the measured charge density (color scale) in a 2D-representation where the x-axis is the time (associated with the applied voltage through the experimental protocol) and the y-axis the position between anode and cathode.

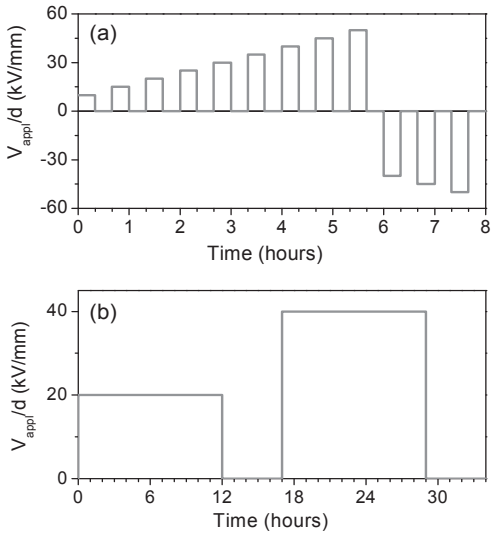

Fig. 2: Short (a) and long (b) term protocols for space charge measurements

III. RESULTS AND DISCUSSION

A. Space charge dynamics and efficiency of barrier to injection in the different samples

The space charge dynamics in a reference sample and in sample S1 (large and isolated particles) was reported in [7] along the protocol shown in Fig. 2a. The space charge dynamic in different samples is shown in Fig. 3 during the 20 min of the 50 kV/mm step. Space charge in the reference sample is governed by injection of positive charges from the SC/LDPE

Table I: Experimental parameters for silver sputtering and characteristics of deposited AgNPs.

Sample	Input power (W)	Argon pressure (Pa)	Density of AgNPs NPs/cm²	Covered area	Size distribution (nm)	Shape and organization	SEM images
S1	40	8.00	6.1×10^{11}	65%	15 ± 10 nm	Large isolated	
S2	40	5.33	7.7×10^{11}	64%	< 10 nm	Small isolated	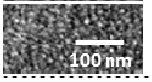
S3	60	8.00	2.0×10^{11}	74%	22 ± 15 nm	Large isolated	
S4	60	5.33	6.3×10^{11}	75%	14 ± 10 nm	Large isolated	
S5	80	8.00	1.8×10^{11}	88%	30 ± 10 nm	Large coalesced	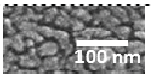
S6	80	5.33	4.4×10^{11}	85%	21 ± 10 nm	Large isolated	

contact and its migration into the bulk. In opposite, positive charge injection cannot be evidenced in the tailored sample S1, with large and isolated AgNPs. Negative charge injection from the Al/polymer contact is evidenced and the whole distribution is dominated by negative space charge. This behavior indicates a strong barrier effect for charge injection due to the nanocomposite layer. Space charge dynamics is also shown for sample S2 (small isolated AgNPs), S5 (large coalesced clusters) and S0 (organosilicon layer without AgNPs). Each distribution exhibits specific features with equivalent amount of heterocharge in S2, a predominance of negative heterocharge in S5 and a predominance of positive heterocharge in S0. A simplified description of the arisen physical situation is presented on the sketch of space charge represented in Fig. 3. Each contact is injecting positive (anode) and negative (cathode) charges (stage 1). Charges migrate towards the electrode of opposite polarity and the net charge detected by the PEA is zero in the middle of the sample due to mutual compensation, under the assumption of a perfect symmetry between injection and transport parameters for the electrons and holes (stage 2). In a third stage, heterocharge can form if there is an unbalance between the incoming charge flux and the extraction flux which seems to be the case in our experiments (semi-blocking electrode [14]). In reality, there is no reason to observe symmetry between injection and transport parameters for both kinds of charges. In the reference sample, there is a massive dissymmetry between injection of positive and negative charges: the SC/LDPE contact is an efficient emitter for holes and negative injection from the contact Al/LDPE is not observed. In sample S1, the nanocomposite layer provides an efficient barrier for hole injection and one observes negative charge injection from the Al/polymer interface. In sample S2, the situation is quite balanced between positive and negative charge injection and transport with an equivalent amount of heterocharge at both electrodes (same trend in sample S0 which is the organosilicon matrix without AgNPs). Sample S5 exhibits more negative heterocharge than positive one. Overall, the above description offers a criterion to compare the efficiency of the barrier to injection for positive charges in each sample. Because the charges originate only from injection, the sign and the amount of charges accumulated in the vicinity of the cathode is a measure of the efficiency of the contact SC/sample for positive injection. We have averaged the charge density accumulated at the end of each voltage step of the short term protocol from 40 µm to 100 µm from the cathode for every tested sample. The results are plotted in Fig. 4. Following this scheme, ranking the barrier efficiency to injection for positive charge is the following: S1 (large isolated clusters 15 nm) > S4 (large isolated clusters 14 nm) > S5 (large coalesced) > S3 (large isolated 22 nm) > S0 (organosilicon matrix) > S2 (small isolated < 10 nm) and the reference. The barrier effect is therefore efficient for non-percolated Ag-clusters of 15 nm in size, and less efficient or failing when the nanoparticles are smaller or percolated.

B. Polarity effect and long term behaviour

A sample, tailored at both sides, in the conditions of sample S1 (large and isolated AgNPs) has been prepared to verify the above stated criterion. As can be seen in Fig. 3 (sample quoted DS), there is no indication of positive or negative charge injection from the contacts (both electrodes are SC contacts to avoid the complexity in the analysis when using contact of different natures). The barrier effect is therefore operative in both polarities.

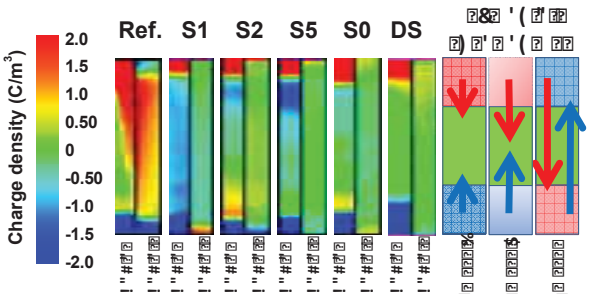

Fig. 3: Representation of the space charge dynamics at 50 kV/mm along the short term protocol in polarization (20 min) and depolarization (20 min): reference LDPE (ref); sample S1 (large and isolated clusters); S2 (small and isolated clusters); S5 (large and percolated clusters); S0 (organosilicon matrix without nanoclusters); DS (tailored on both sides in the conditions of S1).

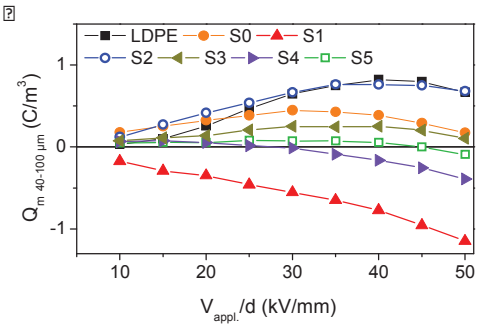

Fig. 4: Charge density averaged from 40 µm to 100 µm from the cathode at the end of each voltage step for the different tested samples

The long term behavior has been investigated following the long term protocol for samples Ref., S1, S2 and S5. We used the same criterion for comparing the barrier efficiency in the different samples as before, plotting the amount of charge accumulated from 40 µm to 100 µm from the cathode at different times during the application of the 40 kV/mm step. As can be seen from Fig. 5 the barrier effect is operative on the long term stress with the same ranking between the different samples.

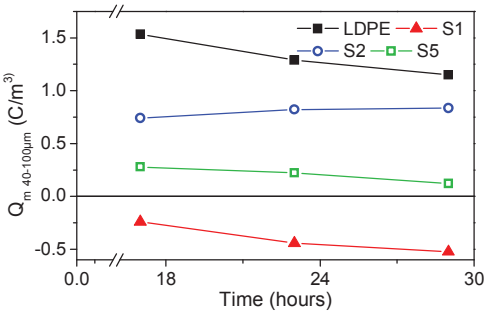

Fig. 5: Charge density averaged from 40 µm to 100 µm from the cathode during the 40 kV/mm step along the long term protocol

C. Discussion

At least three features of the AgNPs have to be considered to read the detected charge injection mitigation effect: the average size of the AgNPs, their surface density and the fact they can be isolated or percolated. Owing to the experimental results, the surface density does not seem to be a critical factor in the range of densities investigated here; to the least inter-connection and size of particles appear more influential. The average particles size is influential with less pronounced mitigation effect when it is lower than 10 nm (S2) when compared to 15 nm (S1) or 14 nm (S4). AgNPs in sample S3 (22 nm, isolated clusters) and S5 (30 nm, percolated clusters) have higher average size and appear also as less efficient in mitigating charge injection than in S1 (15 nm) and S4 (14 nm). It appears therefore, that the AgNPs optimum size for efficient charge injection mitigation is about 15 nm.

Another experimental fact is that the charge mitigation by the AgNPs is observed under both polarities of the applied voltage. Quantum effects due to the size reduction would hardly give an interpretation for the polarity effect and are not in agreement with the experiments (clusters of size < 10 nm are less efficient than larger clusters). An alternative would be to consider the stability of charged clusters. By using different metal cluster generation and ionization methods, it has been shown that some charged clusters are more stable than others depending on the number of constituting atoms [15]. These so-called "magic numbers" were successfully explained by shell like arrangement of electrons in the cluster, so that the cluster achieves a higher stability at shell closing. Little is known about the stability of multiple charged clusters, even if stable triple charged silver ions (Ag_n^{3+}) have been observed for specific values of n. In each case, the higher stability was explained by the electronic occupation of shells. Both silver clusters anions [16] and cations [15] have been observed and this could give a basis for the interpretation of the barrier to injection effect observed under both voltage polarities. However, the average size of the Ag-clusters in our nanocomposite layer (estimated to be 3×10^4 atoms and 1×10^5 atoms for 10 nm and 15 nm cluster diameter, respectively) is much higher than the upper limit for conventional DFT quantum computation [17]. But the possibility that they stabilize positive and negative charge has to be considered. A simple field calculation assuming a single charge state of each AgNP in the case of sample S2 leads to a field value at the electrode of 63 kV/mm (with a AgNP density of 7.7×10^{11} cm^{-2} and a relative permittivity of 2.2 for LDPE), which is actually of the order of magnitude of the applied field. Besides, if every AgNP accommodates more than one charge the barrier effect is magnified. A reasonable interpretation of the barrier effect could therefore be a field reduction at the injecting electrode due to AgNPs charging.

IV. CONCLUSION

Charge injection from a semi-conducting electrode into low density polyethylene submitted to a DC field has been investigated up to 50 kV/mm through space charge dynamics. Charge injection is suppressed when non-percolated AgNPs of 15 nm in size are present in the nanocomposite layer. The effect is observed for both polarities of the voltage and for long polarization duration (28 hours). AgNPs appear a key feature for charge injection suppression. The ability for silver clusters to stabilize electrical charges thereby counterbalancing the injecting field seems to be a key factor in explaining charge injection mitigation.

ACKNOWLEDGMENT

The authors acknowledge support from the UMS Raymond Castaing of the University of Toulouse and thank Mr. Stéphane Le Blond du Plouy for the SEM observations.

REFERENCES

[1] T.L. Hanley, R.P. Burford, R.J. Fleming and K.W. Barber, "A general review of polymeric insulation for use in HVDC cables", IEEE Electr. Insul. Mag., 19, 13-24, 2003.

[2] M.S. Khalil, "International research and development trends and problems of HVDC cables with polymeric insulation", IEEE Electr. Insul. Mag., 13, 35-47, 1997.

[3] G.C. Montanari and P.H.F. Morshuis, "Space charge phenomenology in polymeric insulating materials", IEEE Trans. Dielectr. Electr. Insul. 12, 754-767, 2005.

[4] C. Laurent, G. Teyssedre, S. Le Roy and F. Boudoin, "Charge dynamics and its energetic features in polymeric materials", IEEE Trans. Dielectr. Electr. Insul., 20, 357-381, 2013.

[5] T. Tanaka and T. Imai, "Advances in nanodielectric materials over the past 50 years", IEEE Electr. Insul. Mag., 29, pp. 10–23, 2013.

[6] Z. An, Q. Yang, C. Xie, Y. Jiang, F. Zheng and Y. Zhang, "Suppression effect of surface fluorination on charge injection into linear low density polyethylene", J. Appl. Phys., 105, 064102, 2009.

[7] L. Milliere, K. Makasheva, C. Laurent, B. Despax and G. Teyssedre, "Efficient barrier for charge injection in polyethylene by silver nanoparticles/plasma polymer stack", Appl. Phys. Lett. 105, 122908, 2014.

[8] L Milliere, K Makasheva, C. Laurent, B. Despax, L. Boudou and G. Teyssedre, "Effects of a modified interface by silver nanoparticles/SiOC:H barrier layer against space charge injection under HVDC", Proc. IEEE Conference on Electrical Insulation and Dielectric Phenomena (CEIDP) 2014, pp. 883-886, 2014.

[9] S. Le Roy, G. Teyssedre, C. Laurent, C. Montanari and F. Palmieri, "Description of charge transport in polyethylene using a fluid model with a constant mobility: fitting model and experiments", J. Phys. D: Appl. Phys. 39, 1427-1436, 2006.

[10] B. Despax and P. Raynaud, "Deposition of polysiloxane thin films containing silver particles by an RF asymmetrical discharge", Plasma Process. Polym., 4, 127–134, 2007.

[11] K. Makasheva, C. Villeneuve-Faure, S. Le Roy, B. Despax, L. Boudou, C. Laurent, and G. Teyssedre "Silver nanoparticles embedded in dielectric matrix: charge transport analysis with application to control of space charge formation", Proc. IEEE Conference on Electrical Insulation and Dielectric Phenomena (CEIDP) 2013, pp. 238-241, 2013.

[12] C. Laurent and E. Kay, "Properties of metal clusters in polymerized hydrocarbon versus fluorocarbon matrices" J. Appl. Phys., 65, 1717-1723, 1989.

[13] K. Fukunaga and T. Maeno, "Internal space charge measurement for the study of the electrostatic phenomena", J. Electrostatics, 40-41, 431-435, 1997.

[14] S. Le Roy, G. Teyssedre, C. Laurent, L.A. Dissado and G.C. Montanari, "Relative Importance of Trapping and Extraction in the Simulation of Space Charge Distribution in Polymeric Insulators under DC Potentials", Proc. 2007 International Conference on Solid Dielectric (ICSD), pp. 494-497, 2007.

[15] I. Rabin, C. Jackschath, and W. Schulze, "Shell effects in singly and multiply charged silver and gold clusters", Z. Phys. D - Atoms, Molecules and Clusters 19, 153-155, 1991.

[16] A. Herlerta, L. Schweikhard, and M. Vogel, "Observation of multiply charged silver-cluster anions", Eur. Phys. J. D16, 65-68, 2001.

[17] N.D.M. Hine, P.D. Haynes, A.A. Mostofi, C.K. Skylaris, M.C. Payne, "Linear-scaling density-functional theory with tens of thousands of atoms: Expanding the scope and scale of calculations with ONETEP", Computer Phys. Comm., 180, 1041-1053, 2009.